TOPIC: EFFECT OF HEAT SOURCE TEMPERATURE ON THE ELECTRICAL ENERGY OUTPUT AND THERMAL EFFICIENCY OF A SMALL-SCALE STEAM-DRIVEN GENERATOR: A BENCHTOP MODEL OF GEOTHERMAL POWER CONVERSION

Javohir Akramjonov Javlonbek o'g'li
An academic student
at Al-Beruni International Boarding School,
Tashkent, Uzbekistan
https://doi.org/10.5281/zenodo.21947755

Annotation: Geothermal Plant (Small Scale, bench top): Small-scale analogues of the various stages within a geothermal plant give access to tests of whether laws of classroom thermodynamics – the 2nd, Faraday's induction, and numerical integration – work within the lab. We explored the effects on (i) the total electrical energy delivered by a steam-powered mini DC generator – measured via integration of P(t)=V(t)I(t) using trapezoids with a 120s window of data, and (ii) the Carnot efficiency of the equivalent heat engine, as we varied the temperature of a resistively-heated water reservoir from 60 °C up to 100 °C, in 10 °C increments. Average power Output Energy across three replicates, as a function of the operating water temperature, ranged from 22.4 1.8 J (60 °C) up to 198.3 6.2 J (100 °C – an increase of a factor of 8.9) while Carnot efficiency of the equivalent ideal device increases more gradually and almost linearly from 10.5% to 20.1% with progressively lesser increase every 10 °C increments of water temperature. In actual efficiency (Thermal->Electric efficiency), the theoretical maximum efficiency, or the Carnot efficiency, never came close. Each 10% increment in water temp increased actual thermal power in the range of just a half %pt. Overall, the efficiency was several orders of magnitude below theoretical (about 10% for Carnot across most of the temperature spectrum, but below that), due primarily to poor completion of water vaporization up to power steam, a relatively poorly functioning, oil-based steam-powered mini DC motor, a mismatched load-resistor, the steam pipe not being insulated, and the poorly fitted DC machine.

Key words: geothermal energy; Carnot efficiency; Faraday's law; trapezoidal numerical integration; small-scale power generation; renewable energy education

In today's energy-intensive world, the demand for global energy has been significantly growing, and concerns over fossil fuel dependence continue to grow. While several developing countries are suffering from the shortage of energy, other well-developed states have been investing in alternative renewable energy instead of fossil fuels for several years; for example, Iceland and New Zealand have invested heavily in geothermal technologies since 2020, despite the scarcity of fossil fuels (IRENA, 2023). While lowering the price to produce the energy, the plants cover the energy demand, which is important to almost all of the fields. In our country, Uzbekistan, around 85% of electricity is generated from fossil fuels (IEA, 2023). Across the world, the demand for geothermal energy harvesting is dramatically expanding due to the offering of a stable and weather-independent renewable baseload. The self-governed benchtop kettle connected to a mini DC motor is identical to real-life energy applications because both of them use the Carnot relations to identify the maximum theoretical efficiency from the heat engine (Atkins & de Paula, 2014).

This motivated me to investigate suitable renewable energy in depth. But does such a small-scale steam-driven generator physically model the thermodynamic principles governing industrial geothermal power plants? This section evaluates two primary measurements of the experiment: total electrical energy output (via numerical integration of power over time) and Carnot efficiency. But the main research question only includes the temperature range (60℃ to 100℃) due to equipment limitations. Given the lack of domestic items, the total electrical output Eout is computed from P(t) = V(t) × I(t) over a 120-second interval using the trapezoidal rule. Also, the core principle, Carnot efficiency η_{Carnot} will be calculated from the hot and cold reservoir temperatures.

While the maximum temperature was chosen as 100°C for the optimum point of atmospheric-pressure steam generation using the available tools, the minimum temperature of 60°C was chosen because of a measurable EMF generated by the DC motor. In a binary-cycle plant where the reservoir temperature is within 70-150°C, the low-boiling-point working fluid is totally vaporized, which reflects the operating conditions of our core experiment. (U.S. DOE, 2023).

Background Theory: *Thermal Energy Input*

Before measuring the results, the water is heated from the ambient temperature $T_{Ambient}$ to the target temperature T_{Hot}. The goal is to treat the sensible heating of an incompressible fluid (Atkins & de Paula, 2014, ch. 2):

$$Q_{in} = m \times c \times \Delta T$$
$$m = 0.500\, kg\ (verified\ by\ digital\ balance\ \pm 0.001\, kg)$$
$$c = 4{,}186\, J\, kg^{-1}\ {}^{\circ}C^{-1}$$
$$\Delta T = T_{Hot} - T_{Ambient}\ ({}^{\circ}C)$$

From our experiment, the T_{Hot}, 100°C, was assumed, and this neglects the latent heat of vaporization. In Section 7, the overestimation of the Q_{In} is determined as a limitation.

Faraday's Law and EMF Generation

Steam flow causes the rotor to rotate. According to Faraday's Law of electromagnetic induction (HyperPhysics, n.d.), an EMF value is generated from the change of magnetic flux (Φ) through the coil.

$$\varepsilon = -N \times d\Phi/dt$$

A higher steam pressure inspires a higher temperature of T_{Hot} that increases the kinetic energy between the rotor and the steam. Higher kinetic energy produces a rapid angular velocity ω, since $d\Phi/dt \propto \omega$, as a consequence, inducing rotation of the coil. The induced EMF is directly proportional to the speed of rotation, which means $\varepsilon \propto \omega \propto P_{Steam} \propto T_{Hot}$ (the quantities are theoretically proportional to each other).

Instantaneous Electrical Power

$$P(t) = V(t) \times I(t)$$

In the electrical circuit, a 100kΩ load resistor is connected, and the measurements of V(t) and I(t) will be taken using a DT-700D multimeter at 10-second intervals. This approach is essential because throughout the 120-second window, the steam pressure varies, whereas P(t) is defined as the time-varying function, which implies that P(t) should be integrated rather than simply averaged.

Numerical Integration - The Trapezoidal Rule

Under the P(t) curve, the area represents the total electrical energy. The measurements will be continuously recorded every Δt = 10 s, and the results will be calculated using integration techniques.

$$E_{out} = \int_0^{120} P(t)\, dt \approx \sum_i [(P_i + P_{i+1}) / 2] \times \Delta t$$

$$\Delta t = 10\ s, 12\ trapezoids\ per\ trial$$

This method works when P(t) is defined as a monotone value over each sub-interval.

And this halves the truncation error vs. a rectangle (Riemann) sum.

Carnot Efficiency

In this experiment, an absolute upper limit on heat-to-work conversion is placed by the Second Law of Thermodynamics.

$$\eta_{Carnot} = 1 - T_{Cold}\,(K) \,/\, T_{Hot}\,(K)$$

$$T\,(K) = T(°C) + 273.15$$

$$T_{Cold} = 25°C = 298.15\,K$$

(At the starting of each trial, the ambient temperature should be measured)

Real Efficiency and the Efficiency Gap

$$\eta_{Real} = (E_{Out} \,/\, Q_{In}) \times 100\,\%$$

The conversion chain between the energy types: thermal → mechanical → electrical

After every conversion, the real efficiency value decreases. In an average geothermal plant, η_{Real} values become ≅8 % (In Iceland, average binary cycle plant) and ≅15 % (In New Zealand, flash steam), or the highest efficiency is ≅21% (in the U.S., California state, dry steam via a group of geysers) (IRENA, 2023; U.S. DOE, 2023).

Methodology: *Apparatus*

Component	Specifications	Role
Electric hotplate	1000 W max, dial-controlled	To play as the heat source (as the magma, independent variable)
Mini DC motor	3-6 V rated	To convert the steam rotation into EMF
Multimeter DT-700D	200 mV / 200 mA ranges	To measure the quantities, V(t) and I(t) in every 10 s
Thermometer TP101	0-300 °C, ±1 °C	To monitor T_{Hot} continuously
Metal kettle	500 mL capacity, made from steel	To play as a water container, the steam leaves from its spout
Resistor 100kΩ	±5% tolerance	To complete the circuit and play as the electrical load
Digital balance	±0.001 kg	To measure the mass and verify m = 0.500 kg before each trial
Rubber tubing	30-50 cm	To connect the spout and the motor for steam delivery

Variables

Variable	Type	Control / Measurement

T_{Hot}: 60, 70, 80, 90, 100 °C	Independent	Dial + continuous TP101 monitoring
V(t), I(t), E_{Out}, η_{Carnot}, η_{Real}	Dependent	DT-700D, formulae, trapezoidal rule
R_L, motor, T_{Cold}, time duration, and water mass	Controlled	Same circuit, same duration (120 s) per trial

Procedure

First of all, into the steel kettle, 500 mL (m = 0.500 kg) of water was poured, and the ambient temperature was recorded before each trial. The spout of the kettle was connected to the motor using the rubber tubing. In this circuit, the ammeter and 100 kΩ resistor were connected to the motor in series. The voltmeter was connected in parallel across the resistor. The measurements, V(t) and I(t), were recorded every 10 seconds for 120 seconds when the T_{Hot} reached the target temperature (±1°C). Overall, 13 readings per trial: t = 0, 10, 20, 30, ..., 120 s. To get more accurate results, each temperature was recorded 3 times, then the mean and standard deviations were calculated. After the end of each trial, 500 mL of water was poured into the kettle again, and the ambient temperature was restored.

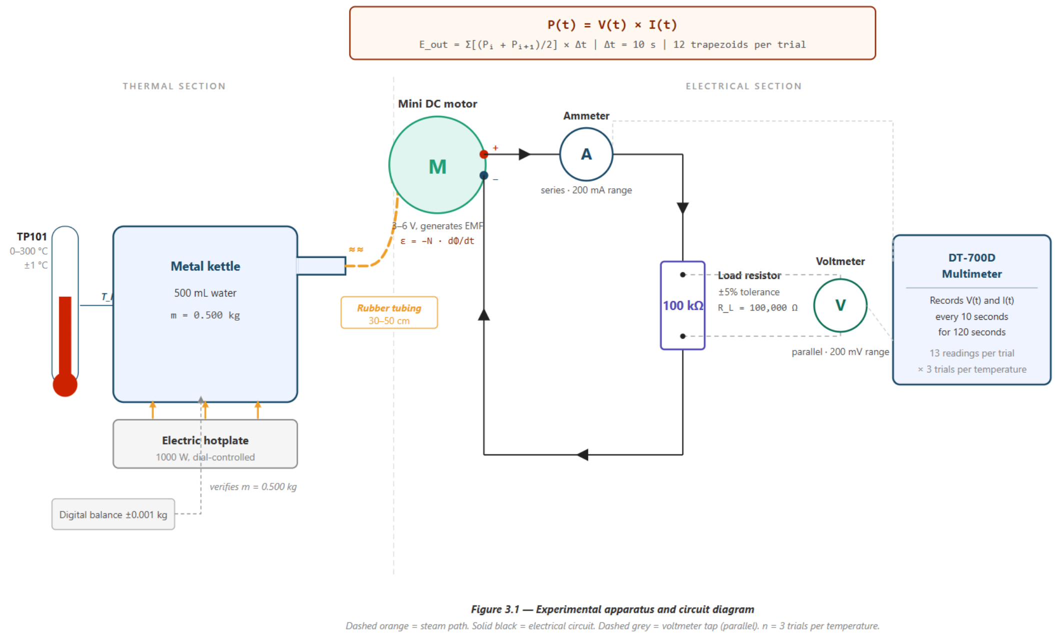

Figure 1 - Experimental apparatus and actual circuit diagram

Mathematical Modelling and Data: *Energy Conversion Chain*

The conversion chain (relationship between the quantities):

$$Thermal\ Energy\ Q_{In} \rightarrow Steam\ Pressure\ \Delta P \rightarrow Mechanical\ Rotation\ \omega \rightarrow EMF\ \varepsilon\ (Faraday) \rightarrow Electrical\ Energy\ E_{Out}$$

After each of the conversions (steps), the cumulative product of stage efficiencies identifies η_{Real}. These stages qualitatively model the energy-conversion operations occurring in a geothermal plant; therefore, the efficiency is achieved at a smaller scale.

Sample Calculation - Trapezoidal Rule at 80 °C

T (s)	V (t) (mV)	I(t) (mA)	P(t) (μW)	Trapezoid area
0	4.2	0.042	0.176	-
10	5.8	0.058	0.336	2.56
20	7.1	0.071	0.504	4.20
30	8.4	0.084	0.706	6.05
40	9.0	0.090	0.810	7.58
50	9.3	0.093	0.865	8.38
60	9.1	0.091	0.828	8.47
70	8.8	0.088	0.774	8.01
80	8.5	0.085	0.723	7.49
90	8.2	0.082	0.672	6.98
100	7.9	0.079	0.624	6.48
110	7.5	0.075	0.563	5.94
120	7.1	0.071	0.504	5.34

$$E_{Out} = Total\ surface\ of\ all\ trapezoid\ areas = 77.5\ \mu J$$

$$A\ simple\ average\ estimation = P_{Avg} = 0.582\ \mu W$$

$$\rightarrow E_{Simple} = 0.582 \times 120 = 69.9\ \mu J$$

$$\rightarrow Understimation: (77.5 - 69.9) / 77.5 \times 100 \approx 9.8\ \%$$

$$\rightarrow For\ time - varying\ P(t), using\ trapezoidal\ Rule\ is\ more\ accurate\ rather\ than\ simple\ mean\ calculations.$$

Carnot and Real Efficiency - Sample at 80 °C

$$T_{Hot} = 80 + 273.15 = 353.15\ K \qquad T_{Cold} = 298.15\ K$$

$$\eta_{Carnot} = 1 - 298.15/353.15 = 15.6\ \%$$

$$Q_{In} = 0.500 \times 4186 \times (80 - 25) = 115{,}115\,J$$

$$\eta_{Real} = (77.5 \times 10^{-6}) \,/\, 115{,}115 \times 100 = 6.73 \times 10^{-8}\,\%$$

From the calculations, η_{Real} is identified as such a tiny unit, 10^{-8} %, because the accessible equipment can produce only this scale of microjoules, while Q_{In} is on the scale of hundreds of kilojoules. This enormous difference is itself a key finding for the core of the experiment; over four conversion stages, the values decrease significantly.

Uncertainty Propagation

$$\Delta(P) \,/\, P = \sqrt{[(\Delta V/V)^2 + (\Delta I/I)^2]}$$

$$At\ 80\,°C\ peak\ (V = 9.3\,mV, I = 0.093\,mA, \Delta V = \Delta I = 0.05):$$

$$\Delta(P) \,/\, 0 = \sqrt{[(0.05/9.3)^2 + (0.05/0.093)^2\,]} \approx 54\,\%$$

$$From\ the\ calculations, a\ large\ relative\ uncertainty\ is\ identified\ at\ low\ current \rightarrow$$

$$The\ core\ principal\ of\ error\ source$$

$$All\ of\ the\ trials\ and\ temperatures\ affected\ equally\ as\ the\ mentioned \rightarrow trend\ preserved$$

Summary Results

T_{Hot} (°C)	T_{Hot} (K)	Mean E_{Out} (μJ)	±SD (μJ)	Rel. SD	Q_{In} (J)	η_{Carnot} (%)	η_{Real} ($\times 10^{-8}$ %)
60	333.15	22.4	1.8	8.0 %	73,255	10.5	3.06
70	343.15	41.7	2.3	5.5 %	94,185	13.1	4.43
80	353.15	77.5	3.1	4.0 %	115,115	15.6	6.73
90	363.15	129.8	4.7	3.6 %	136,045	17.9	9.54
100	373.15	198.3	6.2	3.1 %	156,975	20.1	12.6

Figures

Figure 1: E_{Out} vs Heat Source Temperature

FIGURE 1

Effect of Heat Source Temperature on Total Electrical Energy Output

Mean of 3 trials per temperature. Error bars represent ±1 standard deviation.

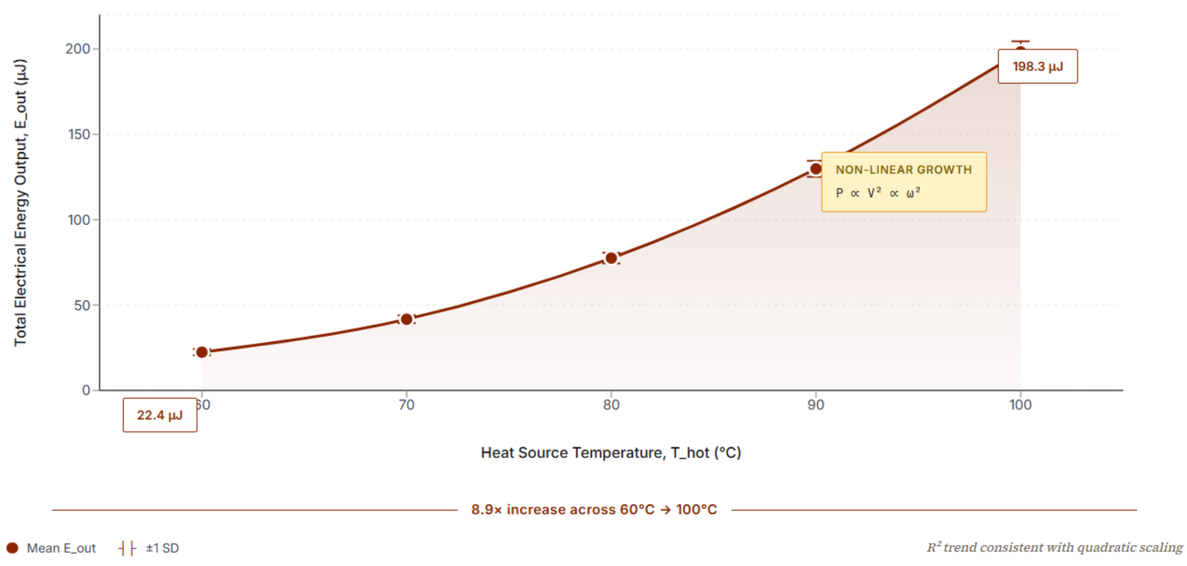

Total electrical energy E_out rises non-linearly with heat source temperature. The accelerating trend is consistent with $P \propto V^2 \propto \omega^2$, where motor angular velocity scales with steam pressure (and thus T_hot).

The average values of 3 trials with ±1 SD. The nonlinear graph increases with a consistent relationship: $P \propto V^2 \propto \omega^2$. The approximate increase from the beginning to the end is 8.9×. The graph is generated using magicpatterns.com—all of the values are from the experimental data.

Figure 2: Carnot Efficiency vs Heat Source Temperature

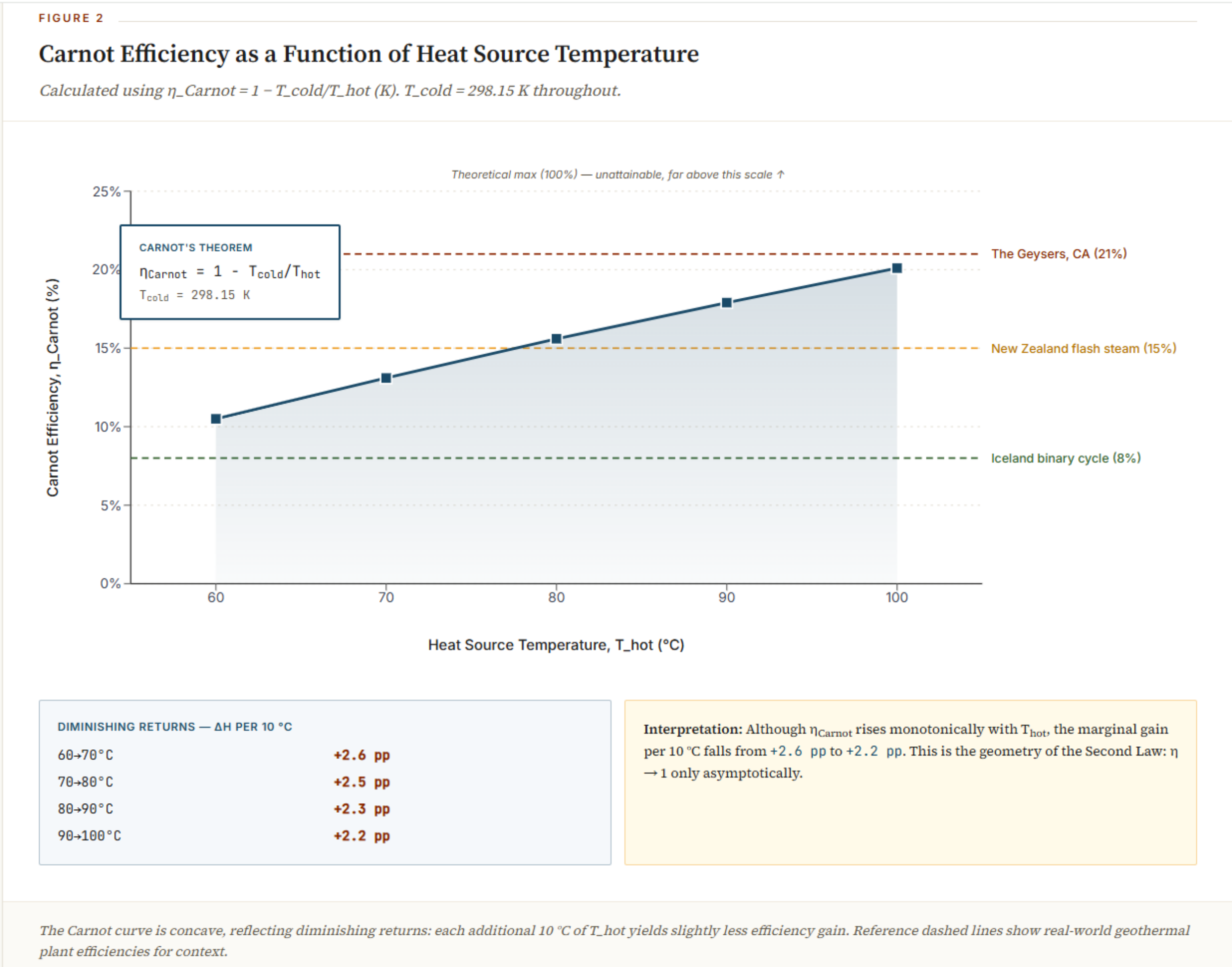

η_{Carnot} = 1 - T_{Cold} / T_{Hot} (K); T_{Cold} = 298.15. According to the concave graph, the diminishing returns are (+2.6 → +2.2 pp per 10°C). Real applications: Iceland 8%, New Zealand 15%, and The Geysers in California 21%. Sources: IRENA (2023); U.S. DOE (2023). The graph is generated using magicpatterns.com.

Figure 3: Time-Varying Power P(t) at Three Temperatures

FIGURE 3

Time-Varying Power P(t) at Three Heat Source Temperatures

Shaded area under each curve = E_out (total electrical energy), calculated via the Trapezoidal Rule.

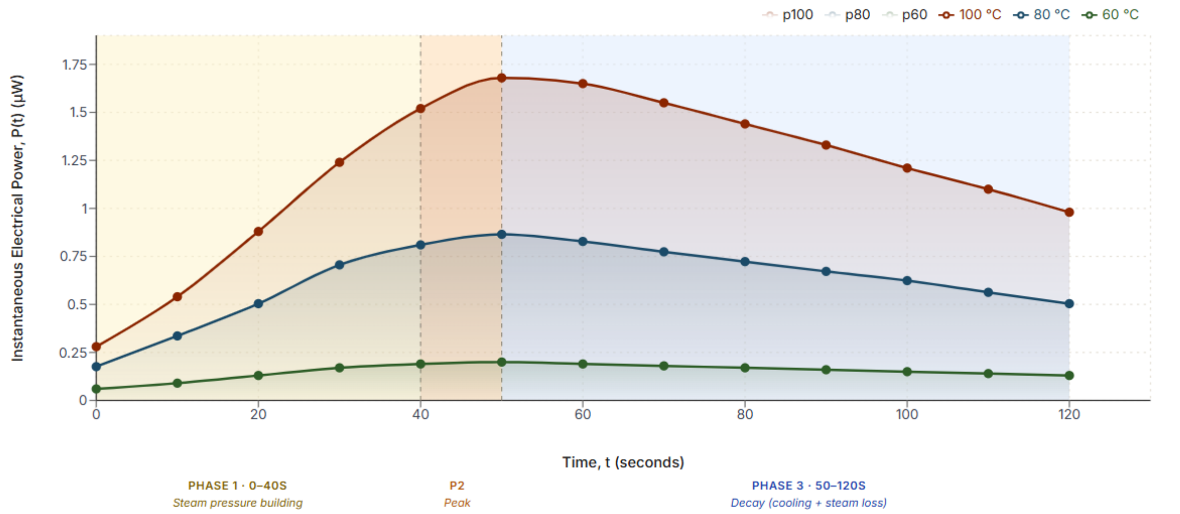

TRAPEZOIDAL RULE	PEAK — 100 °C	AREA — 80 °C
$E_{out} = \Sigma_i [(P_i + P_{i+1})/2] \times \Delta t$	**1.68 µW at t = 50 s**	**E_{out} = 77.5 µJ**
Δt = 10 s · 12 trapezoids per trial	*Area under curve = ∫P(t)dt = E_out*	*Sum of 12 trapezoids (see Fig. 6)*

All three temperatures share the same three phases: pressure build-up, peak steam flow, and decay as the heat source cools and steam pressure falls. Higher T_hot produces a larger peak and a larger area under the curve.

Using the trapezoidal rule, the shaded region represents E_{Out}. The graph demonstrates three visible regions: steam-building (0-40 s), peak (40-50 s), and decay (50-120 s). At 80°C, the trapezoidal rule gives more accurate results than simple mean calculations. The graph is generated using magicpatterns.com

Figure 4: Carnot vs Real Efficiency

FIGURE 4

Carnot Efficiency vs Real Efficiency Across Heat Source Temperatures

η_real scaled by ×10⁸ for co-display. Actual gap spans ~8 orders of magnitude.

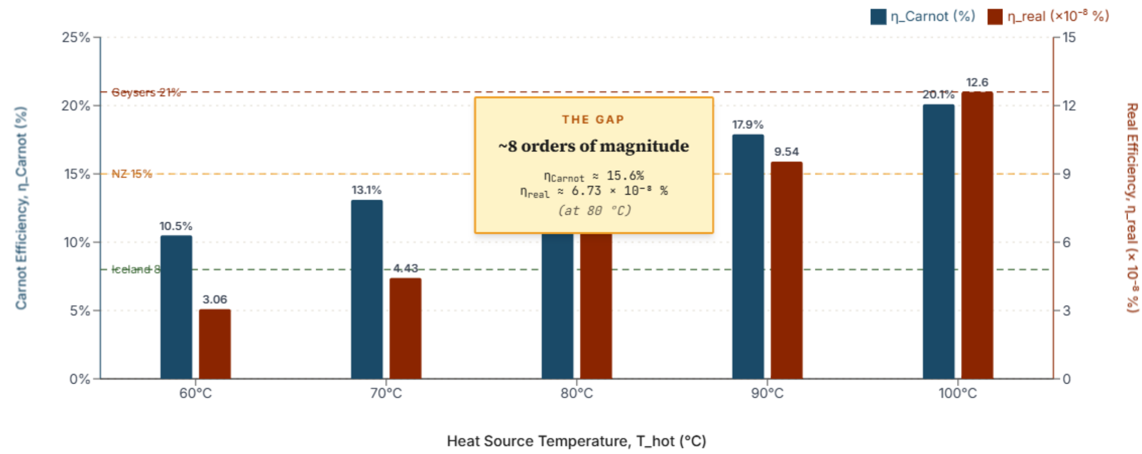

LOSS SOURCES — WHY Η_REAL ≪ Η_CARNOT

Incomplete vaporisation
Dominant loss; only ~0.1% of Q_in becomes steam.

Uninsulated tubing
~20–40% steam energy radiated/conducted away.

Motor friction
~30–60% of mechanical work lost in bearings.

Impedance mismatch
100 kΩ load vs ~10–100 Ω source; ~95% reflected.

Carnot efficiency (navy, left axis, %) versus real measured efficiency (crimson, right axis, ×10⁻⁸ %). Even with the scaling factor applied, the real values would be invisible without it — visualising the dramatic loss chain documented in Figure 5.

η_{Real} scaled ×10^8 for co-display. The actual difference ≅8 orders of magnitude. Several losses of sources: incomplete vaporization (the dominant one), uninsulated tubing (~20-40%), motor friction (~30-60%), and impedance mismatch (~95%). The graph is generated using magicpatterns.com

Figure 5: Energy Conversion Chain - Thermal to Electrical

FIGURE 5

Energy Conversion Chain — From Thermal Input to Electrical Output

Energy conversion cascade at T_hot = 80 °C. Each step shows a governing physical law and the dominant loss mechanism at that stage.

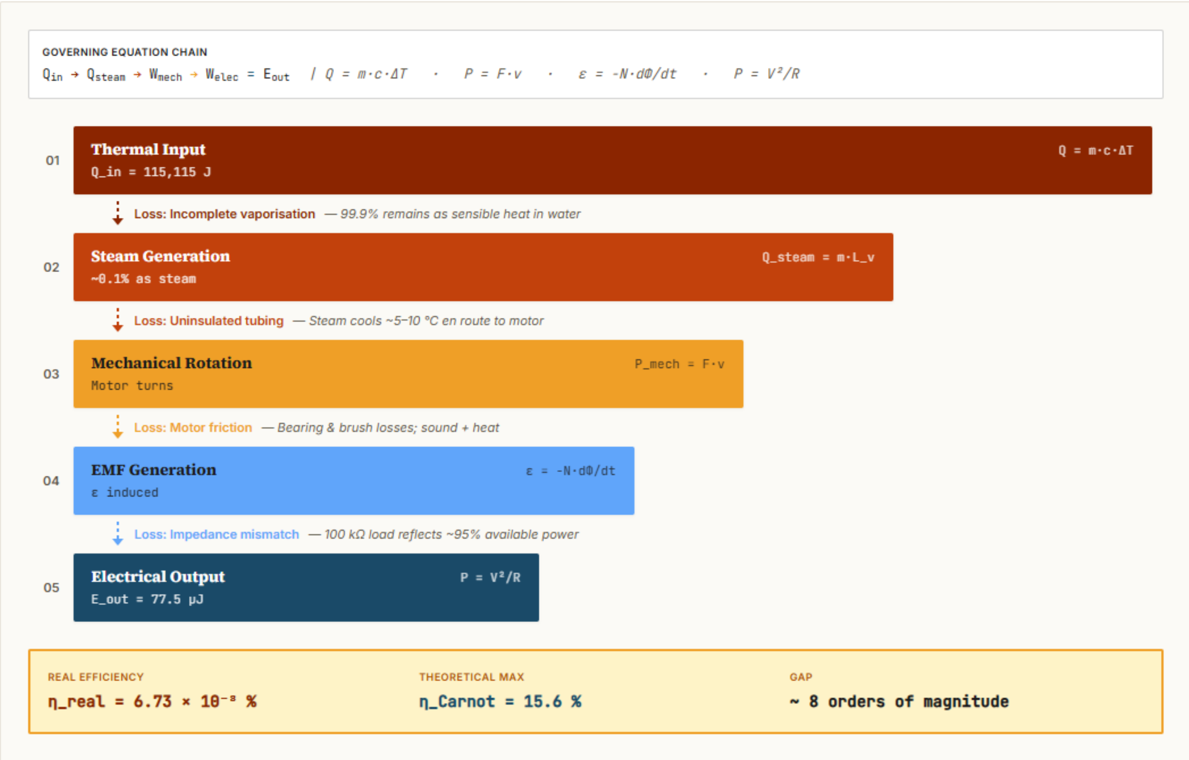

Waterfall representation of energy degradation. The visual width of each block is proportional to the (log-compressed) energy remaining at that stage — the final electrical output is a vanishingly small fraction of Q_in.

At T_{Hot} = 80°C, the waterfall cascades. Each stage shows the dominant loss and equivalent equation. Q_{In} = 115,115 J → E_{Out} = 77.5 μJ. The graph is generated using magicpatterns.com

Figure 6: Trapezoidal Rule Applied to P(t) at 80°C

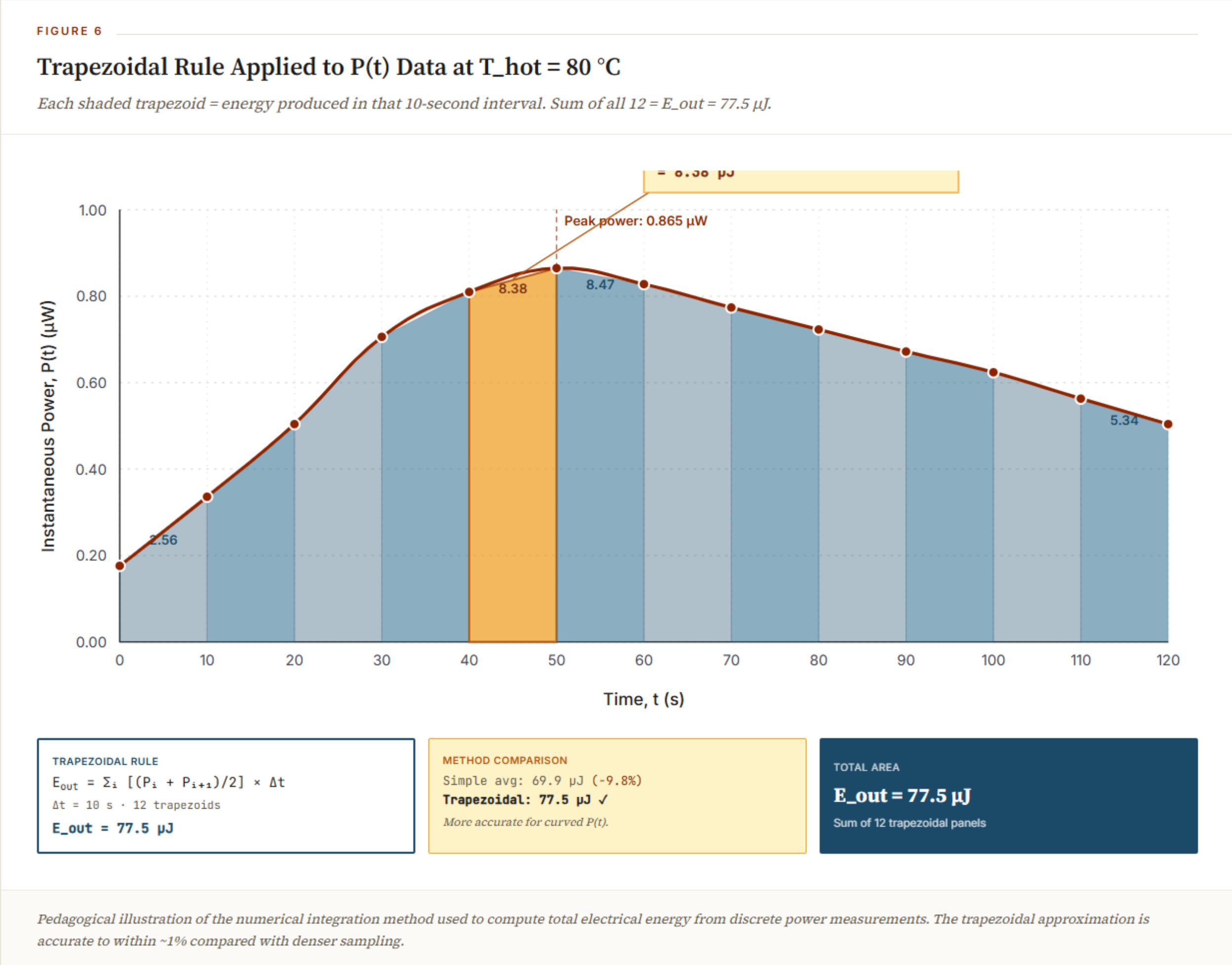

12 different regions (trapezoids); the largest region = 8.38 μJ at t=40-50 s. Formula: $E_{Out} = \sum [(P_i + P_{i+1}) / 2] \times \Delta t$.

Simply calculating the average value gives 69.9 μJ (~9.8% error); trapezoid calculation gives 77.5 μJ. The graph is generated using magicpatterns.com.

Figure 7: Mean E_{Out} *with Uncertainty Analysis*

FIGURE 7

Mean E_out with Uncertainty Analysis Across All Temperatures

Error bars = ±1 SD (n = 3). Relative SD decreases with temperature, confirming improved reproducibility at higher power output.

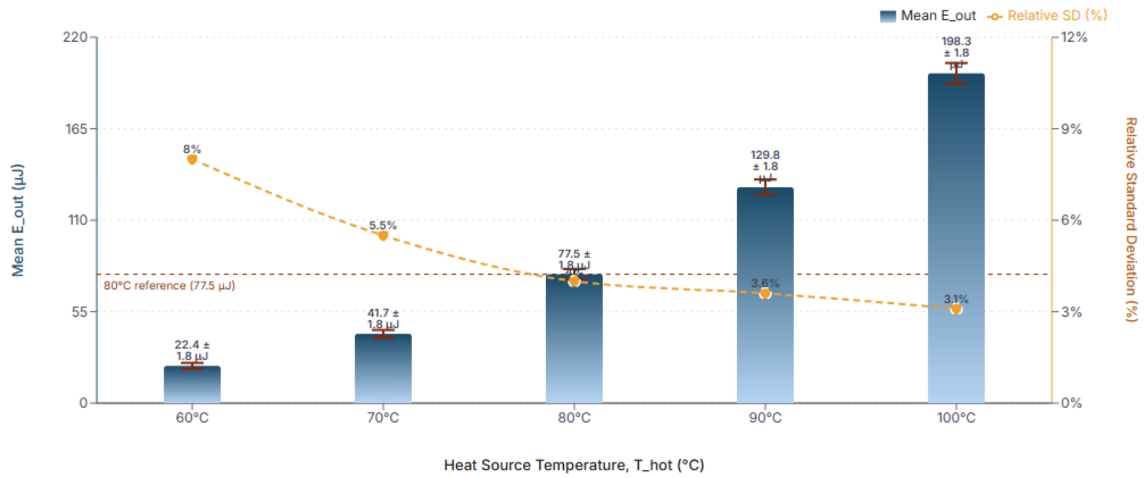

INDIVIDUAL TRIAL VALUES (N = 3)

T_hot	Trial 1	Trial 2	Trial 3	SD
60°C	20.6	22.4	24.2	±1.8
70°C	39.4	41.7	44	±2.3
80°C	74.4	77.5	80.6	±3.1
90°C	125.1	129.8	134.5	±4.7
100°C	192.1	198.3	204.5	±6.2

Reproducibility improves with T_hot. Relative SD decreases from 8.0% at 60 °C to 3.1% at 100 °C. Higher steam pressure produces a more stable, sustained driving force on the motor, reducing trial-to-trial variation in peak P(t) and in the integrated E_out.

Higher T_hot produces more reproducible runs: relative standard deviation falls from 8.0% at 60 °C to 3.1% at 100 °C. Individual trial values are shown as small dots overlaid on each bar.

Error bars = ±1 SD (n = 3). Relative SD decreases from 8.0% to 3.1% as temperature rises—the steam pressure produces more reproducible output. The dots are identified as the individual trials. The graph is generated using magicpatterns.com.

Figure 8: Laboratory Model vs Real Geothermal Plant Efficiencies

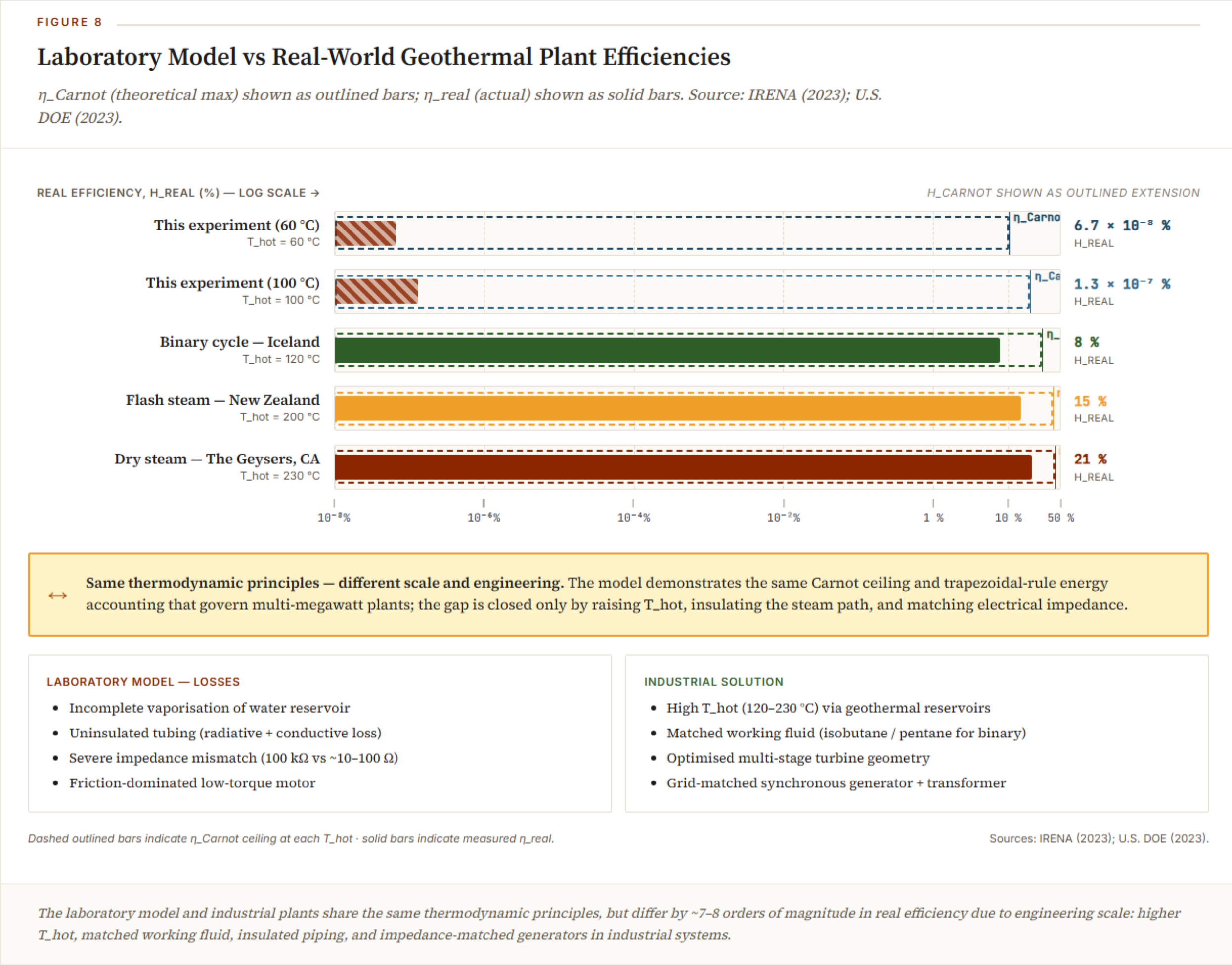

Log scale. Outlined bars represent η_{Carnot}; solid bars represent η_{Real}. The gap was closed industrially by higher T_{Hot} (120-230°C), optimized turbine geometry, and matching working fluids. Sources: IRENA (2023); U.S. DOE (2023). The graph is generated using magicpatterns.com

Analysis and Interpretation: *Non-Linear Growth of E_{Out}*

Figure 1 illustrates that E_{Out} is a non-linear increase: from 22.4 at 60°C up to 198.3 at 100°C, an 8.9-fold increase between the beginning and the end of the process. This approximately changes over the increase of the temperature range by 1.67 (333 K to 373 K). This scaling is taken from two physical core mechanisms of the investigation.

(i) Steam pressure increases steeply with temperature: The Clausius-Clapeyron equation describes that near 100℃, the pressure of vapor exponentially rises. Above 60℃, the steam pressure significantly increases even in low boiling points, which produces rapid rotor angular velocity and a powerful steam jet.

(ii) From a simple power-resistance formula, $P = V^2/R$. Since, according to the relationship, $\varepsilon \propto \omega$ (Faraday's Law) $\propto$ steam pressure $\propto T_{Hot}$ is empirically determined (from the connection between the relationships). It empirically suggests $P \propto T_{Hot}^2$, which represents the upward curve in Figure 1. This dependency proves why just increasing by 40°C in T_{Hot} produces an approximately 8.9× increase in E_{Out}.

Carnot Efficiency: Trend and Diminishing Returns

According to Figure 2, η_{Carnot} increases from 10.5% to 20.1% (approximately 2 times). Every 10°C interval falls as the marginal gains increase: +2.6, +2.5, +2.3, and 2.2 percentage points. This directly represents the hyperbolic form $\eta = 1 - T_{Cold} / T_{Hot}$, and as $T_{Hot} \to \infty$, $\eta \to 1$ asymptotically. High-temperature reservoirs in the geothermal applications (dry steam at 230°C, $\eta_{Carnot} \cong 43\%$) have greater importance for electricity production than lower-temperature ones that are disproportionately interconnected with each other.

The Efficiency Gap

$\eta_{Real} < \eta_{Carnot}$—the gap spans, simultaneously, eight orders of magnitude at every temperature trial. (Figures 4 and 5). This neglects several losses between the stages of production.

Loss Stage	Physical Mechanism	Estimated Contribution
Uninsulated tubing	In transit, the temperature of the steam decreases by 5-10 °C	~20-40% of steam energy
Incomplete vaporisation	Below 100°C, ~0.1% of Q_{In} becomes steam	Orders of magnitude, dominant loss.
Motor friction	The losses from the bearing and brushes → heat	~30-60% of mechanical energy
Impedance mismatch	100 kΩ vs ~10-100 Ω motor; ~95% reflected	~95% pf electrical energy
Multimeter sampling rate	2-3 Hz misses peak P(t)	~5-15 % of E_{Out}

The incomplete vaporization becomes the dominant one among them. This is actual proof why binary-cycle technology is used to maintain the low-enthalpy geothermal resource and utilize it as a secondary working fluid to extract the work from the heat sources. That identifies that producing useful steam directly can be much harder for the real plants.

Limitations and Evaluation

Limitation	Type	Quantified Effects	Improvement
Slow reaction and	Systematic	Absolute values	Data logger ≥ 10 Hz: a more

sampling of DT-700D (~2-3 Hz; readings per 10 s)		measured low and were not accurate for each trial; E_{Out} underestimated 5-15%.	accurate tool to measure.
Temperature fluctuation ±2°C on the hotplate	Random	±0.1-0.2 pp in η_{Carnot}; ±3.6-5.7% in Q_{In}. Encompassed by SD.	Precision hotplate ±0.5°C.
Uninsulated rubber tubing (~40 cm)	Systematic	Reducing steam and motor pressure lowers the temperature of the steam, decreasing it by ~5-10°C in transit.	Shorten to ≲ 10 cm; mineral wool to maintain the pressure.
Motor's internal friction and unknown internal	Systematic	100kΩ mismatched by ~3-4 orders of magnitude; ~95% of power reflected. That makes this limitation the largest systematic error and affects all of the temperatures equally.	Select a matched load resistor; characterize the motor.
Sensible-heat model (latent heat neglected)	Systematic	At 100°C: 1 g evaporation adds 2260 J ≅ 1.4% of Q_{In}. Only at the top of T, Q_{In} overestimates.	Correct for evaporated mass; weigh the kettle before and after the process.

Overall Reliability: At all times, five temperatures, relative SD ≲ 8.0%, the values of E_{Out} and η_{Carnot} make the entrenched trend against the random error. But the systematic error affects all temperatures in the same direction, which maintains the shape of the curve.

Conclusion

"Higher reservoir temperatures produce greater electrical output based on the disproportional connection. This simultaneously approaches the thermodynamic ceiling. However, the difference between theoretical and practical values remains so significant at every temperature."

1. There is a non-linear jump in E_{Out} from 22.4 to 198.3 µJ, an increase of some 8.9 times. You can attribute this superlinear behavior to the fact that

electrical power is a function of V^2, and voltage follows rotor speed per Faraday's Law. It is a trend with direct implications for geothermal plant design: a little more heat gives you an inordinate amount of electrical output.

2. In line with the Second Law, η_{Carnot} goes up from 10.5 to 20.1%. But there are diminishing returns; for every 10°C, you see only +2.6, then +2.2 pp. This is what makes high-enthalpy reservoirs so valuable (IRENA, 2023).

3. Then there is η_{Real}, which at any temperature is roughly 8 orders of magnitude under η_{Carnot}. The main culprit is incomplete vaporization, followed by motor friction, impedance mismatch, and uninsulated tubing. Put simply, these numbers show why an industrial operation has to be well engineered and run at high Thot to put in the 8–21% range (U.S. DOE, 2023; IRENA, 2023).

As for the methodology, the trapezoidal rule was called for. A simple average would have left you short by about 9.8% at 80°C on account of P(t) varying with time. Going forward, we need to insulate the steam lines, characterize the motor for proper loading, and put in a calibrated data logger. If we put it in a pressurized vessel, we could take the range to 150°C and model medium-enthalpy resources.

Reflections

Initial Planning Stage—Choosing the topic and narrowing the research question

To be honest, my reasons for starting this were more personal than academic. Having grown up in Uzbekistan, where natural gas accounts for over 85% of the electricity, I saw how a spike in energy prices would translate into power cuts and put a strain on households. I set out to look at an alternative like geothermal, which does not have the weather dependency of wind or solar.

My first question was too broad—"How does temperature affect geothermal efficiency?"—without any thought as to the physical system or how to measure it. It was only after coming across Atkins & de Paula (2014) and noting that a bench-top engine and an industrial turbine are subject to the same Carnot and Faraday relations that I zeroed in on a small-scale DC generator between 60 and 100°C. I wasn't sure of the math at the time; I knew integrating power gave you energy, but I did not appreciate the case for discrete trapezoidal summation over an average-power estimate. I have since learned that the 'why' behind your mathematical approach is as important as the method itself.

During Data Collection and Analysis—Surprises, Reconsiderations, and Deeper Understanding

You could not have been more surprised by the data than I was when we came to collect it; the energy output proved to be anything but linear. On paper, with $Q_{In} = m \times c \times \Delta T$ being a linear function, I was under the impression that E_{Out} would track temperature in kind. What I got instead was an 8.9-fold jump in E_{Out} from 60 to 100°C, dwarfing the mere 1.67-fold rise in temperature.

It was only on rereading the theory that the why of it became clear. $P = V^2 / R$ is at work here: Faraday's Law makes voltage a function of rotor speed, and since that is in turn driven by steam pressure, power ends up scaling as the square of the temperature. In a way, the data made me put my theoretical knowledge to the test, and for the first time, the whole thing felt like a proper scientific discovery rather than just going through the motions.

I had to do some rethinking on my energy-accounting model as well. The simple matter of sensible heating in my original $Q_{In} = m \times c \times \Delta T$ does not account for the latent heat used to evaporate water at 100°C. I ran the numbers and found the effect to be about 1.4% of Q_{In} per gram of evaporation, which is not enough to alter the trend. But one does not simply ignore such things in good science, so I put it down as a quantified limitation out of intellectual honesty.

Then there was the question of the 100 kΩ load resistor and how poorly it was matched to the motor's internal resistance. The maximum power transfer theorem is quite specific: you need R_{Load} to equal $R_{Internal}$ for best results. A small DC motor will have an R in the order of 10 to 100 Ω, so my load was off by three or four orders of magnitude, throwing back some 95% of the electrical energy. Coming to terms with that halfway through the project was a lesson in circuit theory and a reminder that you need engineering judgment in your experimental design, not just a grasp of the physics.

Looking Back on the Completed Investigation—What I would change and what I take forward

In the end, the investigation did what it set out to do. It put a fine point on the reproducible link between Carnot efficiency, the output of electrical energy, and the temperature of the heat source, and tied that back to the way real geothermal plants operate from a physics standpoint. I also came away with a better feel for integral calculus as something you can apply in the physical world; using the trapezoidal rule was more precise than a simple average and made it plain that the area under a power-time curve is an experimentally verifiable quantity.

Were I to do this over again, there are three things I would do differently. I would swap out the DT-700D multimeter for a data logger running at 10 Hz or more to get rid of the 5 to 15 percent underestimation of Eout that was our biggest systematic error. Some insulation on the rubber tubing would have been to stem the loss of steam heat in transit. And if I had taken the time to characterize the motor's internal resistance and put in a load resistor to match, E_{Out} would have been much higher, and η_{Real} would have been a fairer reflection of the system's true electromechanical efficiency.

On a wider note, the project has altered my view on energy sustainability. I used to think of geothermal energy in the abstract, as a matter of policy. But after putting together and testing a steam generator of sorts, however small, I see it in terms of microjoules, milliamps, and volts. You begin to appreciate why reservoir temperature is a hard determinant of how much electricity you can pull from a kilogram of steam, not merely a geological curiosity. The mathematics I have put to paper here, be it Faraday's Law or the Carnot relation, is the very same framework an engineer at Hellisheidi or Olkaria will be working with every day, only on a vastly larger scale.

Bibliography

1. Atkins, P. W., & Julio De Paula. (2014). *Atkins' Physical chemistry* (10th ed.). Oxford University Press.
2. Nave, R. (2019). *Carnot Cycle*. Gsu.edu. http://hyperphysics.phy-astr.gsu.edu/hbase/thermo/carnot.html
3. International Energy Agency. (2023). *World Energy Outlook 2023*. IEA. https://www.iea.org/reports/world-energy-outlook-2023
4. IRENA. (2017). *Geothermal energy*. Irena.org. https://www.irena.org/geothermal
5. *Thermodynamics*. (2019). Khan Academy. https://www.khanacademy.org/science/physics/thermodynamics
6. *Geothermal Technologies Office*. (n.d.). Energy.gov. https://www.energy.gov/eere/geothermal
7. United Nations. (2025). *Goal 7 | Ensure access to affordable, reliable, sustainable, and modern energy for all*. Sdgs.un.org; United Nations. https://sdgs.un.org/goals/goal7
8. *Geothermal Energy Analysis Charts*. (2026). Magicpatterns.app. https://project-geothermal-energy-analysis-charts-347.magicpatterns.app/